

Numerical analysis of the Balitsky-Kovchegov equation with running coupling: dependence of the saturation scale on nuclear size and rapidity

J. L. Albacete^{1,2}, N. Armesto², J. G. Milhano^{2,3}, C. A. Salgado² and
U. A. Wiedemann²

¹ *Departamento de Física, Módulo C2, Planta baja, Campus de Rabanales,
Universidad de Córdoba, 14071 Córdoba, Spain*

² *Department of Physics, CERN, Theory Division, CH-1211 Genève 23, Switzerland*

³ *CENTRA, Instituto Superior Técnico (IST),
Av. Rovisco Pais, P-1049-001 Lisboa, Portugal*

We study the effects of including a running coupling constant in high-density QCD evolution. For fixed coupling constant, QCD evolution preserves the initial dependence of the saturation momentum Q_s on the nuclear size A and results in an exponential dependence on rapidity Y , $Q_s^2(Y) = Q_s^2(Y_0) \exp[\bar{\alpha}_s d(Y - Y_0)]$. For the running coupling case, we re-derive analytical estimates for the A - and Y -dependences of the saturation scale and test them numerically. The A -dependence of Q_s vanishes $\propto 1/\sqrt{Y}$ for large A and Y . The Y -dependence is reduced to $Q_s^2(Y) \propto \exp(\Delta' \sqrt{Y + \bar{X}})$ where we find numerically $\Delta' \simeq 3.2$. We study the behaviour of the gluon distribution at large transverse momentum, characterizing it by an anomalous dimension $1 - \gamma$ which we define in a fixed region of small dipole sizes. In contrast to previous analytical work, we find a marked difference between the fixed coupling ($\gamma \simeq 0.65$) and running coupling ($\gamma \sim 0.85$) results. Our numerical findings show that both a scaling function depending only on the variable $r Q_s$ and the perturbative double-leading-logarithmic expression, provide equally good descriptions of the numerical solutions for very small r -values below the so-called scaling window.

1 Introduction

High-density QCD [1] – the regime of large gluon densities – provides an experimentally accessible testing ground for our understanding of QCD beyond standard perturbation theory. The Balitsky-Fadin-Kuraev-Lipatov (BFKL) equation [2,3] is the perturbative framework in which the evolution of parton densities with decreasing Bjorken- x (increasing energy) is usually discussed. In the BFKL equation it is implicitly assumed that the system remains dilute throughout evolution and hence correlations between partons can be neglected. The fast growth of the gluon density predicted by the BFKL equation and experimentally observed at HERA, eventually leads to a situation in which individual partons necessarily overlap and, therefore, finite density effects need to be included in the evolution. These effects enter the evolution non-linearly, taming the growth of the gluon density.

The need for and role played by saturation effects was first discussed in [4,5]. It was later argued [6–8] that in the high-density domain a hadronic object (hadron or nucleus) can be described in terms of an ensemble of classical gluon fields, and that the number of gluons with momenta smaller than the so-called saturation scale, is as high as it may be (i.e. saturated). The quantum evolution of the hadronic ensemble can be written in terms of a non-linear functional equation [9–15] where the density effects are treated non-perturbatively (see also [16,17]).

An alternative approach, followed by Balitsky [18], relies on the operator product expansion for high-energy QCD to derive a hierarchy of coupled evolution equations (see [19] for a more compact derivation). In the limit of a large number of colours, the hierarchy reduces to one closed equation. This equation was derived independently by Kovchegov [20] in the dipole model of high-energy scattering [21–23].

The relation between these two approaches has been extensively discussed [13–15,24–27]. Apart from possible differences between the evolution equations in the kinematical region where the projectile becomes dense [24], the different approaches yield the same result, usually known as the Balitsky-Kovchegov (BK) equation. This equation has served as the starting point for a large number of analytical and numerical studies. It has also been derived in the S -matrix approach of [28], and as the large- N_c limit of the sum of fan diagrams of BFKL ladders [29,30]. It corresponds, as BFKL, to a re-summation of the leading terms in $\alpha_s \ln(s/s_0)$ (leading-log approximation).

Although the full analytical solution of the BK equation is not known, several of its general properties, such as the existence and form of limiting solutions, have been identified in both analytical [31–37] and numerical [29, 38–43] studies. Most of them refer to the fixed coupling case without impact parameter dependence, but analyses of the effect of a running coupling [42, 44–48] and of the dependence on impact parameter [49–51] have also been carried out. Besides, there have been attempts to go beyond the large- N_c limit, either by analytical arguments [52–54] or by numerically solving the full hierarchy of evolution equations [47]. In this latter work, non-leading N_c corrections are found to give a contribution smaller than 10 ÷ 15%, in qualitative agreement with what could be naively expected from a numerical correction of $\mathcal{O}(1/N_c^2)$. From a phenomenological point of view, studies of the BK equation are motivated by the geometrical scaling phenomenon observed in lepton-proton [55] and lepton-nucleus data [56, 57] which has been related to the scaling properties of the solution of the BK equation (see e.g. [58, 59] for recent numerical analyses of HERA data based on non-linear evolution). Further interest comes from the study of nuclear collisions [60], where saturation physics is argued [61] to underlie a large body of data including multiplicity distributions [57, 62–66] and the rapidity dependence of the Cronin effect [43, 67–70].

Next-to-leading-log contributions [71, 72] are known to have a strong impact on the BFKL equation [73–77]. Both the choice of scale in the coupling constant [78] and the implementation of kinematical cuts for gluon emission [42, 79, 80], together with physically motivated modifications of the kernel [81–83], have been proposed to mend some observed pathologies of next-to-leading-log BFKL. It is usually expected that the unitarity corrections included in the BK equation become of importance for parametrically smaller rapidities [74, 75] than those for which running coupling effects must be included [84]. This can only be definitively established once next-to-leading-log contributions are fully computed for BK (see [85] for a first step in this direction). However, the inclusion of running coupling effects in BK may offer a hint of some of the effects induced at next-to-leading-log, as has been previously the case for BFKL. It may also help to reconcile the results of the equation with phenomenology [45, 57].

In this paper we investigate numerically the influence of the running coupling on the solution of the BK equation without impact parameter dependence, leaving this last point for a future publication. We go beyond previous numerical studies [42, 46, 47] by making a detailed comparison between analytical estimates and our numerical solution

of the BK equation, and analyzing the Y - and A -dependence of the saturation scale. Our key results are the confirmation of the Y - and A -dependence of the saturation scale proposed analytically [32–34], and the novel finding that the anomalous dimension (extracted for dipole sizes smaller than the inverse saturation scale) is different in the fixed and running coupling cases. To compare to analytical results which have been derived for asymptotically large energies, we shall evolve numerically to very large rapidities (up to $Y \sim 80$), significantly beyond the experimentally accessible range.

The plan of the paper is as follows. We first introduce the BK equation in Section 2 and the different implementations of the running of the coupling constant in Section 3. In Section 4 we explain the numerical method used to solve the BK equation. In Section 5 we present our numerical results, and we compare with previous numerical works and with analytical estimates. Finally, we summarize and discuss our main conclusions.

2 The Balitsky-Kovchegov equation

The BK equation gives the evolution with rapidity $Y = \ln(s/s_0) = \ln(x_0/x)$ of the scattering probability $N(\vec{x}, \vec{y}, Y)$ of a $q\bar{q}$ dipole with a hadronic target, where \vec{x} (\vec{y}) is the position of the q (\bar{q}) in transverse space with respect to the center of the target. We define

$$\vec{r} = \vec{x} - \vec{y}, \quad \vec{b} = \frac{\vec{x} + \vec{y}}{2}, \quad \vec{r}_1 = \vec{x} - \vec{z}, \quad \vec{r}_2 = \vec{y} - \vec{z}. \quad (1)$$

If one neglects the impact parameter dependence (which is justified for $r \ll b$, i.e. an homogeneous target with radius much larger than any dipole size to be considered), the BK equation reads ($r \equiv |\vec{r}|$)

$$\frac{\partial N(r, Y)}{\partial Y} = \int \frac{d^2 z}{2\pi} K(\vec{r}, \vec{r}_1, \vec{r}_2) [N(r_1, Y) + N(r_2, Y) - N(r, Y) - N(r_1, Y)N(r_2, Y)], \quad (2)$$

where the BFKL kernel is

$$K(\vec{r}, \vec{r}_1, \vec{r}_2) = \bar{\alpha}_s \frac{r^2}{r_1^2 r_2^2}, \quad \bar{\alpha}_s = \frac{\alpha_s N_c}{\pi}. \quad (3)$$

The coupling constant is fixed and the kernel is conformally invariant. This implies that no impact parameter can be generated if not present in the initial condition. Also, there is no divergence for $r_1, r_2 \rightarrow 0$ provided $N(r, Y) \propto r^\beta$ for $r \rightarrow 0$ with $\beta > 0$.

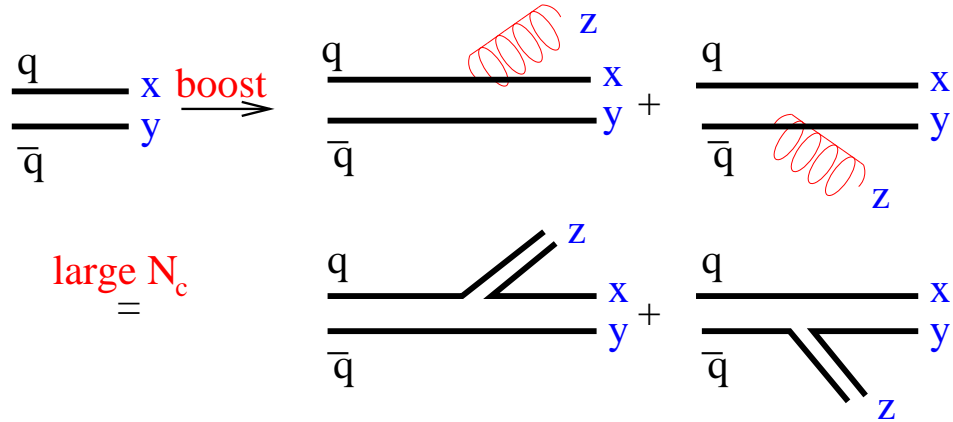


Figure 1: Diagrams for gluon emission in the evolution of a dipole and its $N_c \rightarrow \infty$ limit.

This comes from the cancellation between real and virtual corrections inherited from the BFKL equation. The azimuthally symmetric form of the BFKL equation, which gives the dominant contribution at high energies, corresponds to Equation (2) without the non-linear term.

The BK equation has the following probabilistic interpretation [24] (see Figure 1): when evolved in rapidity, the parent dipole with ends located at \vec{x} and \vec{y} emits a gluon, which corresponds in the large- N_c limit to two dipoles with ends (\vec{x}, \vec{z}) and (\vec{z}, \vec{y}) , respectively. The probability of such emission is given by the BFKL kernel (3), and weighted by the scattering probability of the new dipoles minus the scattering probability of the parent dipole (as the variation with rapidity of the latter is computed). The non-linear term is subtracted in order to avoid double counting. It is this non-linear term which prevents, in contrast to BFKL, the amplitude from growing boundlessly with rapidity. The BK equation ensures unitarity locally in transverse configuration space, $|N(r, Y)| \leq 1$. This is guaranteed since for $N(r, Y) = 1$, the derivative with respect to Y in (2) cannot be positive.

3 Running coupling

The BK equation (2) was derived at leading order in $\alpha_s \ln(s/s_0)$ for a fixed coupling constant α_s . An important part of the next-to-leading-log corrections is expected to come, as in BFKL, from the running of the coupling. The scale of the running coupling can only be determined when the next-to-leading-log calculation is available. In this

paper we introduce heuristically the running of the coupling, as done previously in BFKL (see e.g. [86,87]); we will use different prescriptions for the scales in order to check the sensitivity of the results. To motivate our choices, we recall the interpretation of the BFKL kernel (3) as the Weizsäcker-Williams probability for gluon emission written in a dipolar form,

$$K(\vec{r}, \vec{r}_1, \vec{r}_2) \equiv K_0(\vec{r}, \vec{r}_1, \vec{r}_2) = \frac{\alpha_s N_c}{\pi} \frac{r^2}{r_1^2 r_2^2} = \frac{N_c}{4\pi^2} \left| \frac{g_s \vec{r}_1}{r_1^2} - \frac{g_s \vec{r}_2}{r_2^2} \right|^2, \quad (4)$$

with $g_s = \sqrt{4\pi\alpha_s}$.

Three distance scales appear in this kernel: an ‘external’ one, the size of the parent dipole, r , and two ‘internal’ ones, the sizes of the two newly created dipoles, r_1 and r_2 . The latter depend on the transverse position of the emitted gluon \vec{z} and on \vec{r} through (1). We study three different prescriptions for implementing these scales in a running coupling constant in the BFKL kernel (4):

1. In the first modified kernel, K_1 , the scale at which the running of the coupling is evaluated is taken to be that of the size of the parent dipole, r . This choice amounts to the substitution $\alpha_s \rightarrow \alpha_s(r)$ in Equation (4),

$$K_1(\vec{r}, \vec{r}_1, \vec{r}_2) = \frac{\alpha_s(r) N_c}{\pi} \frac{r^2}{r_1^2 r_2^2}. \quad (5)$$

2. To implement the running of the coupling at the internal scale, we alternatively modify the emission amplitude in (4) before squaring it,

$$K_2(\vec{r}, \vec{r}_1, \vec{r}_2) = \frac{N_c}{4\pi^2} \left| \frac{g_s(r_1) \vec{r}_1}{r_1^2} - \frac{g_s(r_2) \vec{r}_2}{r_2^2} \right|^2. \quad (6)$$

3. In order to check the sensitivity of the results to the Coulomb tails of the kernel, we further modify the kernel K_2 by imposing short range interactions, so that the emission of large size dipoles is suppressed. To do this, we weight the gluon emission vertex by exponential (Yukawa-like) terms,

$$K_3(\vec{r}, \vec{r}_1, \vec{r}_2) = \frac{N_c}{4\pi^2} \left| \frac{e^{-\mu r_1/2} g_s(r_1) \vec{r}_1}{r_1^2} - \frac{e^{-\mu r_2/2} g_s(r_2) \vec{r}_2}{r_2^2} \right|^2, \quad (7)$$

with $\mu = \Lambda_{QCD}$.

Let us anticipate that the different prescriptions K_1 , K_2 and K_3 lead to very similar results for the evolution. This can be traced back to the fact that all the

geometrical dependence on \vec{z} is integrated out so that only the r dependence in the running of the coupling survives. Even the introduction of the exponential damping has little effect, unless the range of the interaction is chosen unphysically small (i.e. $\mu \gg \Lambda_{QCD}$). However, the inclusion of a short range damping effect is known [49, 50] to alter significantly the solution of the BK equation with impact parameter dependence, which we do not consider in the present work.

For the qualitative properties of BK evolution studied in this paper, the precise value and running of the coupling constant is unimportant. To be specific, we use the standard one loop expression

$$\alpha_s(r) = \alpha_s(k = 2/r) = \frac{12\pi}{\beta_0 \ln \left(\frac{4}{r^2 \Lambda_{QCD}^2} + \lambda \right)}, \quad (8)$$

where λ is an infrared regulator and $\beta_0 = 11N_c - 2N_f$ with $N_f = 3$. Both λ and Λ_{QCD} are determined from the conditions $\alpha_s(r = \infty) = \alpha_0$, $\alpha_s(r = 2/M_{Z^0}) = 0.118$, where M_{Z^0} is the mass of the Z^0 boson. In our work, this choice is not motivated by phenomenology, but by its use in related works e.g. [32, 45] to which we want to compare. From now on, when comparing fixed and running coupling results, it will be understood that the value for the fixed coupling is the same as the one at which the running coupling is frozen, α_0 .

4 Numerical method and initial conditions

To solve the integro-differential equation (2), we employ a second-order Runge-Kutta method with a step size $\Delta Y = 0.1$. We discretize the variable $|\vec{r}|$ into 1200 points equally separated in logarithmic space between $r_{min} = 10^{-12}$ and $r_{max} = 10^2$. The numerical values of these limits are dictated by the initial conditions and Λ_{QCD} . Throughout this paper, the units of r will be GeV^{-1} , and those of Q_s GeV . The integrals in (2) are performed with the Simpson method. Inside the grid a linear interpolation is used. For points lying outside the grid with $r < r_{min}$ a power-law extrapolation is used, while for points with $r > r_{max}$ the saturated value of the scattering probability is held constant, $N(r) \equiv N(r_{max}) = 1$. While the initial conditions of $N(r)$ give negligible values for r small but much larger than r_{min} , the evolution leads to a gradual filling of values close to r_{min} with increasing rapidity, which would result eventually in numerical inaccuracies. To solve this problem and push the evolution to very large rapidity, we

rescale, in the fixed coupling case, the variable r in the solutions at intermediate values of Y and use them as initial condition (a power-law extrapolation is used for small values of r in order to cover the r -range lost in the rescaling procedure). In this way, we are able to evolve initial conditions with $Q_s \sim 1$ GeV up to $Y \sim 36$ for $\bar{\alpha}_s = 0.4$ and up to $Y \sim 72$ for $\bar{\alpha}_s = 0.2$. In the running coupling case, the evolution is much slower and this rescaling is not needed to get to large rapidities. The accuracy of our numerical solution for all r -values inside the grid is better than 4% up to the largest rapidities. It is much better than 4% in most of the r -region studied. We have checked this numerical accuracy by varying the step size in Y , by comparing our results to those of a fourth-order Runge-Kutta method, by varying the limits of the grid, by doubling the number of points used to discretize the function in the grid, and by using different integration, extrapolation and interpolation methods.

We evolve three different initial conditions starting from some fixed value of x_0 (in practice one usually takes $x_0 \sim 0.01$). The first initial condition we refer to as GBW since it shows at fixed x_0 the same r -dependence as the Golec-Biernat–Wüsthoff model [88]:

$$N^{GBW}(r) = 1 - \exp \left[-\frac{r^2 Q_s'^2}{4} \right]. \quad (9)$$

However, in contrast to the GBW model [88], our x -dependence comes from BK evolution and we do not impose a power-law parameterization of the x -dependence of Q_s' . Here and in the other initial conditions (10), (11) below, we denote as Q_s' what is usually called the saturation scale. Our definition of the saturation scale Q_s is somewhat different, see Equation (13) below, but the relation between both scales is straightforward e.g. in GBW, $Q_s'^2 = -4 \ln(1 - \kappa) Q_s^2$. The second initial condition takes the form given by the McLerran-Venugopalan model [6, 7] (MV):

$$N^{MV}(r) = 1 - \exp \left[-\frac{r^2 Q_s'^2}{4} \ln \left(\frac{1}{r^2 \Lambda_{QCD}^2} + e \right) \right]. \quad (10)$$

These initial conditions have been used in previous works e.g. [39, 43]. For transverse momenta $k \sim 1/r \geq \mathcal{O}(1 \text{ GeV})$, the sensitivity to the infrared cut off e is negligible. The amplitudes N^{GBW} and N^{MV} are similar for momenta of order Q_s' but differ strongly in their high- k behaviour. The corresponding unintegrated gluon distribution $\phi(k) = \int \frac{d^2 r}{2\pi r^2} e^{i\vec{r}\cdot\vec{k}} N(r)$ decays exponentially for N^{GBW} but has a power-law tail $\sim 1/k^2$ for N^{MV} . As a third initial condition, we consider

$$N^{AS}(r) = 1 - \exp [-(r Q_s')^c]. \quad (11)$$

The interest in this ansatz is that the small- r behaviour $N^{AS} \propto r^c$ corresponds to an anomalous dimension $1 - \gamma = 1 - c/2$ of the unintegrated gluon distribution at large transverse momentum. This anomalous dimension can be chosen to differ significantly from that of the initial conditions N^{GBW} and N^{MV} . Our choices $c = 1.17$ and $c = 0.84$ are somewhat arbitrary. They can be motivated a posteriori by the observation that the anomalous dimension of the evolved BK solution for both fixed and running coupling lies between the anomalous dimension of the initial conditions N^{AS} and N^{GBW} (or N^{MV}). Thus, the choice of N^{AS} is very convenient to establish generic properties of the solution of the BK equation. The values of Q'_s in Equations (9), (10) and (11) are 1.4 GeV for GBW, 4.6 GeV for MV, 0.7 GeV for AS with $c = 1.17$ and 0.6 GeV for AS with $c = 0.84$. These values have been used in all our studies except in those on the A -dependence in Section 5.4, where Q'_s has been rescaled with the nuclear size as discussed in that Section.

5 Results

In this Section, we discuss our numerical results and how they compare to previous numerical work and analytical estimates.

5.1 Evolution: Insensitivity to details of running coupling prescription

Figure 2 shows the evolution of the dipole scattering probability for GBW initial condition with fixed and running coupling. The evolution is much faster for fixed coupling than for running coupling, as already known from previous numerical studies [42,46,47]. Remarkably, the solution is rather insensitive to the precise prescription with which running coupling effects are implemented in the modified BFKL kernels $K1$, $K2$ and $K3$. These differences are very small compared to those between fixed and running coupling.

The small differences arising from the use of different kernels can be understood qualitatively. For example, compared to $K1$, the results obtained for $K2$ are enhanced at small values of r and suppressed at large values of r . This is due to the fact that e.g. for a typical size $\sim 1/Q_s$ of the emitted dipoles r_1, r_2 , a larger size $r > 1/Q_s$ of

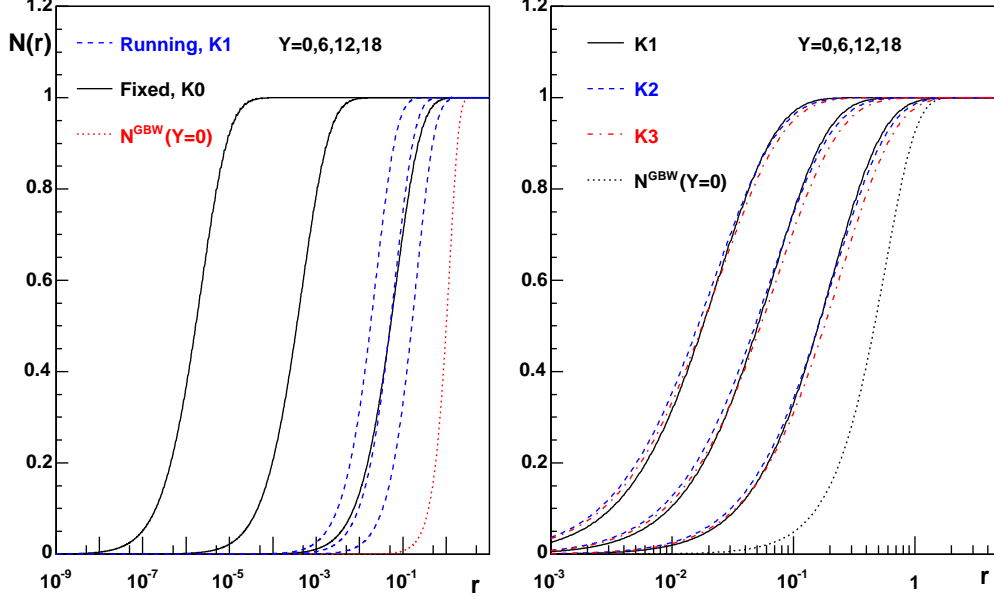


Figure 2: Solutions of the BK equation for GBW initial condition (dotted line) for rapidities $Y = 6, 12$ and 18 with $\bar{\alpha}_0 = 0.4$. Left plot: Evolution with fixed ($K0$, solid lines) and running coupling ($K1$, dashed lines). Right plot: evolution with running coupling for kernel modifications $K1$ (solid lines), $K2$ (dashed lines) and $K3$ (dashed-dotted lines).

the parent dipole amounts to a larger coupling $g_s(r)$ entering the kernel $K1$ than the couplings $g_s(r_1), g_s(r_2)$ entering $K2$. Thus, at large r the evolution is slower for $K2$, which results in the observed relative suppression. The analogous argument implies a relative enhancement obtained from the kernel $K2$ for small $r < 1/Q_s$.

Figure 2 also shows that the effects of imposing short range interactions, $K3$, are very small (unless the range of the interaction is unphysically small). As expected, effects from short range interactions included in $K3$ are larger for larger values of r . It is conceivable that the main next-to-leading-log effects on the original BK kernel are those of the running of the coupling constant included here, and that further modifications, such as kinematical constraints [42, 79, 80], are comparatively small [89].

5.2 Scaling

In the limit $Y \rightarrow \infty$, the solutions of the BK evolution are no longer functions of the variables r and Y separately, but instead they depend on a single scaling variable

$$\tau \equiv r Q_s(Y). \quad (12)$$

Here, the saturation momentum $Q_s(Y)$ determines the transverse momentum below which the unintegrated gluon distribution is saturated. It can be characterized by the position of the falloff in $N(r)$, e.g. via the definition

$$N(r = 1/Q_s(Y), Y) = \kappa, \quad (13)$$

where κ is a constant which is smaller than, but of order, one. We have checked that different choices such as $\kappa = 1/2$ and $\kappa = 1/e$ lead to negligible differences in the determination of $Q_s(Y)$. The results given below have been obtained for $\kappa = 1/2$.

In the fixed coupling case, the scaling property $N(r, Y) \rightarrow N(\tau)$ has been quantified in previous numerical works [39, 41, 43] and confirmed by analytical calculations [35–37]. In the running coupling case, the scale invariance of the BFKL kernel is broken by the scale Λ_{QCD} and it is a priori unclear whether scaling persists. However, when the two scales in the problem are separated widely due to evolution to large rapidity, $Q_s(Y) \gg \Lambda_{QCD}$, one may expect that the scaling property of the BK solution is restored. In agreement with previous numerical works [46, 47], we confirm this expectation: for all modifications $K1$, $K2$ and $K3$ of the BFKL kernel, the solutions tend to universal scaling forms as rapidity increases. Moreover, with increasing rapidity the sensitivity to the choice of scales in the kernel and its short range modification, as well as to the initial condition and to the value of the coupling constant in the infrared, becomes eventually negligible (see Figure 3).

As seen in Figure 3, the shape of the scaling solution differs significantly for fixed and running coupling as observed already in [46]. The running of the coupling suppresses the emission of dipoles of small transverse size (i.e. small τ and large transverse momenta). This leads to an enhancement in the large τ region of $N(\tau)$ which is seen for the running coupling case in Figure 3.

The accuracy of scaling at small r has been studied in a previous work [43] for the fixed coupling case. Here we check scaling for both fixed and running coupling

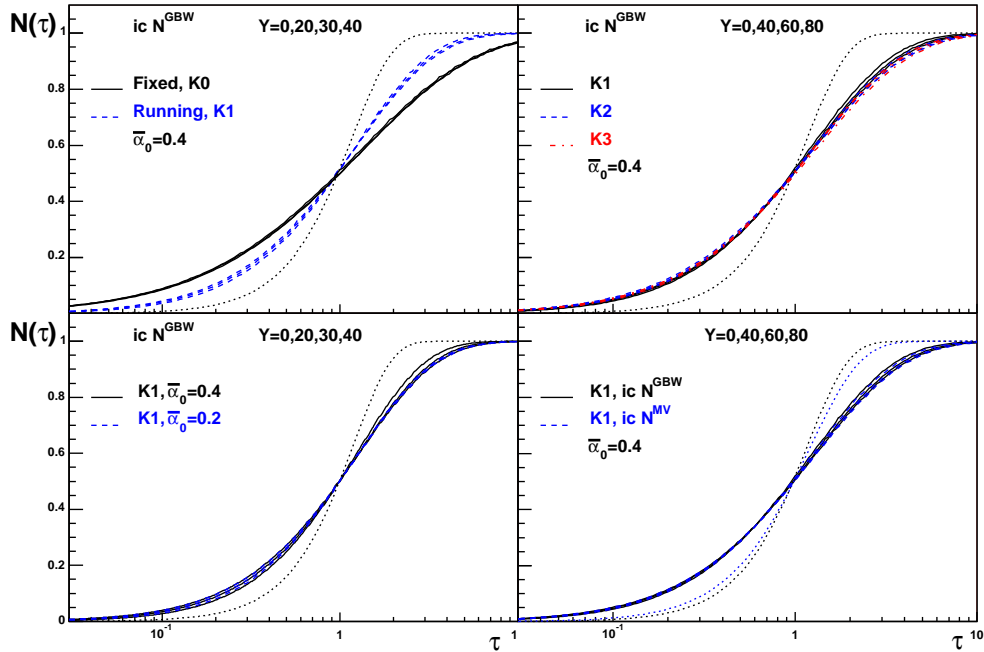


Figure 3: Scaling solutions of BK for $Y = 0, 20, 30$ and 40 (plots on the left) and $Y = 0, 40, 60$ and 80 (plots on the right). Upper-left: evolution for fixed (solid) and running coupling ($K1$, dashed lines) for GBW initial conditions. Upper-right: solutions for the kernels $K1$ (solid), $K2$ (dashed) and $K3$ (dashed-dotted lines). Lower-left: scaling function for $K1$ with two different values of frozen coupling, $\bar{\alpha}_0 = 0.4$ (solid) and $\bar{\alpha}_0 = 0.2$ (dashed lines). Lower-right: scaling solutions with running coupling ($K1$) for two different initial conditions, GBW (solid) and MV (dashed lines). In all plots the initial conditions correspond to the dotted lines and $\bar{\alpha}_0 = 0.4$ unless otherwise stated.

by comparing our numerical results to the scaling forms proposed in Reference [33]. There, it was argued that in the so-called scaling window $\tau_{\text{sw}} < \tau < 1$, the asymptotic solution of $N(r, Y)$ takes the following scaling forms for fixed and running coupling, respectively [33]:

$$f^1(\tau) = a\tau^{2\gamma} \left(\ln \tau^2 + \delta \right), \quad (14)$$

$$f^2(\tau) = a\tau^{2\gamma} \left(\ln \tau^2 + \frac{1}{\gamma} \right). \quad (15)$$

Here, $1 - \gamma$ is usually called the anomalous dimension which governs the leading large- k behaviour of the unintegrated gluon distribution. We define γ from a fit of our numerical results to the functions (14) and (15) in the Y -independent region $10^{-5} < \tau < 10^{-1}$, i.e. for $10^5 Q_s > 1/r > 10 Q_s$, with a , γ and δ as free parameters. The results given below were found to be insensitive to a variation of the lower limit of this

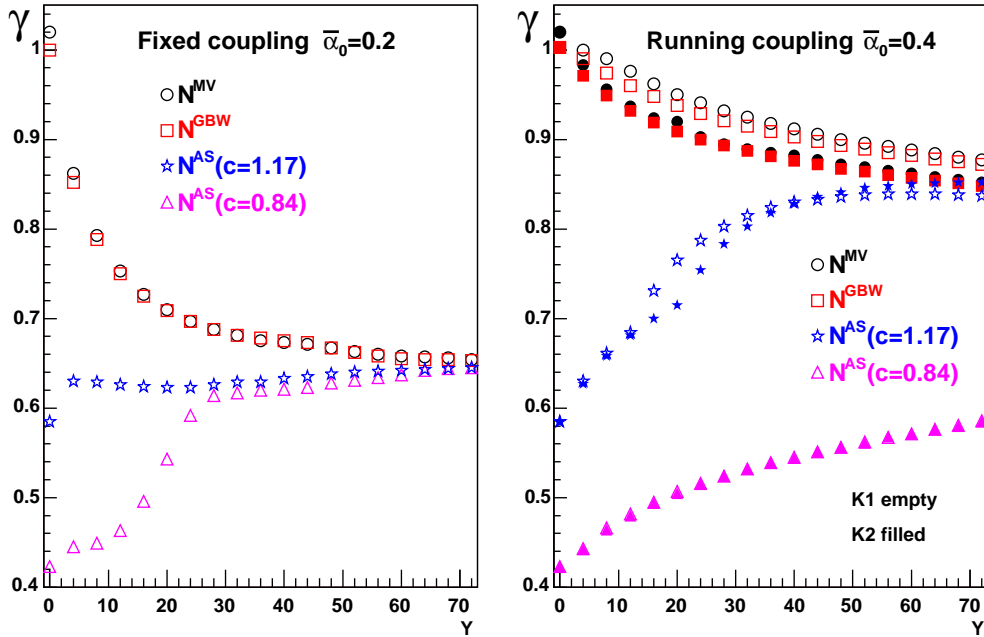


Figure 4: The rapidity dependence of the parameter γ , characterizing the anomalous dimension $1 - \gamma$, as determined by a fit of (14) to the BK solutions for different initial conditions: GBW (squares), MV (circles), and AS with $c = 1.17$ (stars) and $c = 0.84$ (triangles). Left plot: results for fixed coupling with $\bar{\alpha}_0 = 0.2$. Right plot: results for running coupling with $\bar{\alpha}_0 = 0.4$ and two versions of the kernel $K1$ (empty symbols) and $K2$ (filled symbols).

fitting range.

For the case of fixed coupling constant, we find that the function f^1) provides a very good fit to the evolved solutions. In Figure 4, we show the fit values of the parameter γ , obtained for fixed coupling constant from the evolution of different initial conditions N^{GBW} , N^{MV} , and N^{AS} for different values of c . At initial rapidity, these distributions have widely different anomalous dimensions but evolution drives them to a common value, $\gamma \simeq 0.65$, which lies close to the theoretically conjectured one [32,33] of 0.628. For a small fixed coupling constant $\bar{\alpha}_0 = 0.2$, this asymptotic behaviour is reached at $Y \sim 70$, while for a larger coupling constant $\bar{\alpha}_0 = 0.4$ the approach to this asymptotic value takes half the length of evolution (results not shown). For fixed coupling solutions, f^2) does not provide a good fit to our numerical results.

We have repeated this comparison for all running coupling solutions. We found that both f^1) and f^2) provide good fits and yield very similar values of γ . The results for

$K3$ are numerically indistinguishable from those for $K2$ and will not be shown in what follows. Also, the value of γ was found to be independent of the coupling constant $\bar{\alpha}_0$ at $r \rightarrow \infty$. In Figure 4, we show the values of γ extracted from a fit to f^1). Irrespective of the initial condition, they approach a common asymptotic value $\gamma \sim 0.85$. While our numerical findings for N^{AS} with $c = 0.84$ are not inconsistent with the approach to this asymptotic value, no firm conclusions can be drawn. This initial condition just starts too far away from the asymptotic scaling solution to reach it within the numerically accessible rapidity range. In this case, the monotonic increase of γ with rapidity at large Y is smaller than the increase for N^{AS} with $c = 1.17$ at comparable values of γ , indicating that the rapidity evolution of the anomalous dimension depends in general not only on the small- r behaviour, but on the full shape of the scattering probability.

The value $\gamma \sim 0.85$ is considerably larger than the one found in fixed coupling evolution. This is in agreement with previous numerical results [46] but in contrast to theoretical expectations [32, 33, 45] which predict the same value of γ for the fixed and running coupling cases. As an additional check, we have performed running coupling evolution from an initial condition given by the solution at large rapidity of fixed coupling evolution (for which $\gamma \simeq 0.65$). We find that even with this initial condition, running coupling evolution leads to a value of $\gamma \sim 0.85$.

It has been argued [32, 33] that expressions (14) and (15) are only valid for values of τ inside the scaling window, $\tau_{sw} \sim \Lambda_{QCD}/Q_s(Y) < \tau \lesssim 1$ with Y_0 the initial rapidity, and that the dipole scattering probability returns to the double-leading-log (DLL) expression

$$N^{DLL}(r) = a(Y) r^2 [-\ln(r^2 \Lambda^2)]^{-3/4} \exp \left[b(Y) \sqrt{-\ln(r^2 \Lambda^2)} \right], \quad (16)$$

with $a(Y) \propto Y^{1/4}$ and $b(Y) \propto \sqrt{Y}$, for values $\tau < \tau_{sw}$. We have checked that this form provides a good fit (fit and numerical solution differ by less than $\pm 10\%$) to the fixed coupling solution of BK for $\tau < \tau_{sw} = \Lambda/Q_s(Y)$, $\Lambda \sim 0.2$ GeV, see Figure 5. Our comparison is limited to rapidities $Y \leq 20$, since the scaling window starts to extend over the entire numerically accessible r -space for $Y > 20$. Up to $Y = 20$, the coefficients $a(Y)$ and $b(Y)$ follow the expected DLL Y -behaviour, see Figure 5. However, the scaling ansatz f^1) provides an equally good fit to the BK solutions for $\tau < \tau_{sw}$. This is the reason why in previous numerical studies [43] no upper bound for a scaling window was found. When the solutions of BK are fitted to f^1) within the

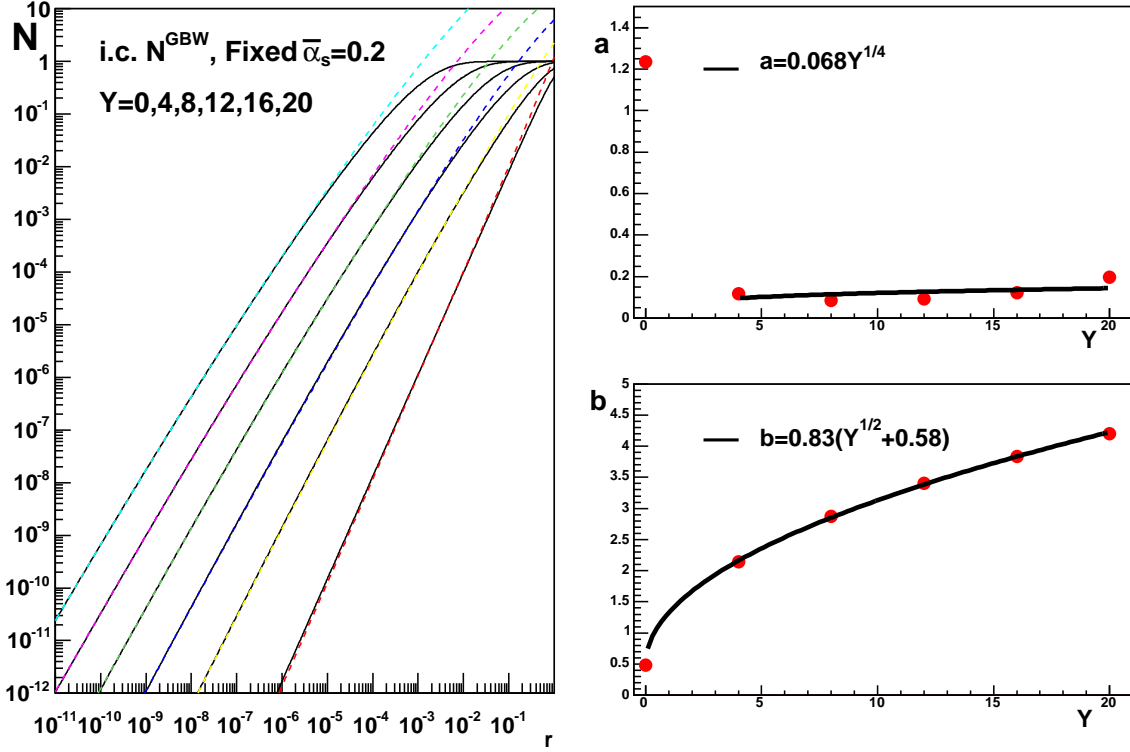


Figure 5: Plot on the left: solutions of the BK equation (solid lines) with GBW initial condition and fixed coupling $\bar{\alpha}_s = 0.2$ compared to fits (dashed lines) to the DLL expression (16), for rapidities $Y = 0, 4, 8, 12, 16$ and 20 (curves from right to left). Plots on the right: values of the coefficients $a(Y)$ and $b(Y)$ (circles) in the DLL expression versus Y , compared to fits (curves) to the functional form suggested by DLL.

scaling window, the values of γ at $Y = 0$ for both initial conditions are $\lesssim 20\%$ smaller than those found when the fit is done within a fixed τ -window. But for larger Y the values of γ extracted from fits within either the scaling window or some fixed τ -window approach each other and quickly coincide.

5.3 Rapidity dependence of the saturation scale

In the scaling region, for large Y where $Q_s(Y) \gg \Lambda_{QCD}$, the BK Equation (2) for fixed coupling constant can be written in terms of the rescaled variables $\vec{\tau} = Q_s(Y)\vec{r}$, $\vec{\tau}_1 = Q_s(Y)\vec{r}_1$ and $\vec{\tau}_2 = Q_s(Y)\vec{r}_2$. The Y -dependence of $N(r, Y) \equiv N(\tau)$ is then contained in $Q_s(Y)$. Rewriting the derivative on the left-hand-side of (2),

$$\frac{\partial N(\tau)}{\partial Y} = \frac{\partial Q_s(Y)}{\partial Y} r \frac{\partial N}{\partial \tau} = \frac{\partial \ln [Q_s^2(Y)/\Lambda^2]}{\partial Y} r^2 \frac{\partial N}{\partial r^2}, \quad (17)$$

one finds [32]

$$\int \frac{d^2r}{r^2} \frac{\partial N(\tau)}{\partial Y} = \pi \frac{\partial \ln [Q_s^2(Y)/\Lambda^2]}{\partial Y} [N(\infty) - N(0)] = \pi \frac{\partial \ln [Q_s^2(Y)/\Lambda^2]}{\partial Y}. \quad (18)$$

Performing the same integration over $d^2r/r^2 = d^2\tau/\tau^2$ on the right-hand-side of (2), one finds a number

$$d = \int \frac{d^2\tau d^2\tau_1}{2\pi^2} \frac{1}{\tau_1^2 \tau_2^2} [N(\tau_1) + N(\tau_2) - N(\tau) - N(\tau_1)N(\tau_2)], \quad (19)$$

which is independent of Y . The numerical value of d cannot be obtained without the knowledge of the scaling solution $N(\tau)$, and several approximations have been proposed [32, 33] which we will compare with our numerical results. Combining Equations (2), (18) and (19), the Y -dependence of the saturation scale is determined [32] by

$$\frac{\partial \ln [Q_s^2(Y)/\Lambda^2]}{\partial Y} = d \bar{\alpha}_s. \quad (20)$$

Thus, for the case of a fixed coupling constant, the saturation scale grows exponentially with rapidity,

$$Q_s^2(Y) = Q_0^2 \exp[\Delta Y], \quad (21)$$

where $\bar{\alpha}_s = \bar{\alpha}_0 = \text{constant}$, $\Delta = d\bar{\alpha}_0$ and $Q_0^2 = Q_s^2(Y=0)$ (i.e. the evolution starts at $Y=0$).

For running coupling, the momentum scale is expected to be $\sim Q_s(Y)$. This suggests the substitution $\bar{\alpha}_s \rightarrow \bar{\alpha}_s(Q_s(Y))$ in Equation (20). To see this explicitly, let us include, as in *K1*, the coupling constant $\bar{\alpha}_s(r)$ in the integrand of (19), which leads to

$$d \bar{\alpha}_s \longrightarrow \frac{12N_c}{\beta_0} \int \frac{d^2\tau d^2\tau_1}{2\pi^2} \frac{1}{\tau_1^2 (\vec{\tau} - \vec{\tau}_1)^2} \frac{1}{\ln [Q_s^2(Y)/\Lambda_{QCD}^2] - \ln(\tau^2/4)} \\ \times [N(\tau_1) + N(|\vec{\tau} - \vec{\tau}_1|) - N(\tau) - N(\tau_1)N(|\vec{\tau} - \vec{\tau}_1|)]. \quad (22)$$

For $\tau \gg 1$, the integrand vanishes. For $\tau \ll 1$, the integral in $d^2\tau_1$ is finite and the remaining $d^2\tau$ suppresses the contribution of small τ . So we conclude that the dominant region is that of $\tau \sim 1$ and thus it is legitimate to approximate

$$\frac{12N_c}{\beta_0} \int \frac{d^2\tau d^2\tau_1}{2\pi^2} \frac{1}{\tau_1^2 (\vec{\tau} - \vec{\tau}_1)^2} \frac{1}{\ln [Q_s^2(Y)/\Lambda_{QCD}^2] - \ln(\tau^2/4)} \\ \times [N(\tau_1) + N(|\vec{\tau} - \vec{\tau}_1|) - N(\tau) - N(\tau_1)N(|\vec{\tau} - \vec{\tau}_1|)] \simeq d \bar{\alpha}_s(Q_s(Y)). \quad (23)$$

This approximation is also supported by numerical results [29, 39, 42] which show that in momentum space the typical transverse momentum of the gluons is $\sim Q_s$. Due to

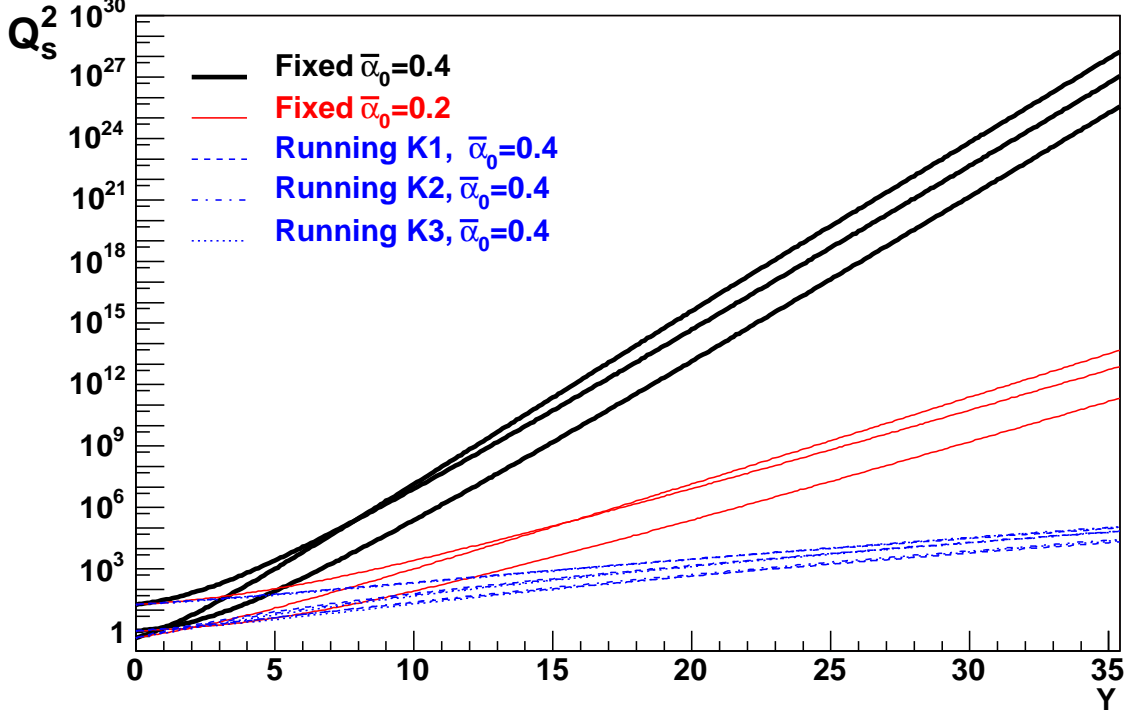


Figure 6: The rapidity dependence of the saturation momentum Q_s^2 for fixed $\bar{\alpha}_s = 0.4$ (thick solid), fixed $\bar{\alpha}_s = 0.2$ (thin solid), and running coupling with $\bar{\alpha}_0 = 0.4$ for kernels $K1$ (dashed), $K2$ (dashed-dotted) and $K3$ (dotted lines). For each group, lines from top to bottom in the rightmost side correspond to initial conditions AS with $c = 1.17$, MV and GBW.

the similarities in the evolution shown previously, this should also hold for other implementation of the scale of the coupling constant such as $K2$ and $K3$. The logarithmic dependence of the coupling constant on $Q_s(Y)$ in (23), combined with Equation (20), leads to [32]

$$Q_s^2(Y) = \Lambda^2 \exp \left[\Delta' \sqrt{Y + X} \right], \quad (24)$$

where $(\Delta')^2 = 24N_c d / \beta_0$ and $X = (\Delta')^{-2} \ln(Q_0^2 / \Lambda^2)$. This estimate indicates that the rapidity dependence of the saturation scale is much weaker for running than for fixed coupling constant.

Figure 6 shows the Y -dependence of Q_s^2 for several initial conditions and different choices of $\bar{\alpha}_0$, calculated for all the kernels considered in this work. The rise of Q_s is much faster for fixed than for running coupling, as already observed in [42,44–48,83,89].

For fixed coupling constant, Q_s^2 exhibits with good accuracy an exponential be-

behaviour for high-enough values of Y . The value of the slope extracted from a fit to the function (21) is $\Delta \simeq 1.83$ for $\bar{\alpha}_0 = 0.4$. As expected, for $\bar{\alpha}_0 = 0.2$ this value is reduced by a factor two, $\Delta \simeq 0.91$. For the constant (19), we find $d \simeq 4.57$, in agreement with previous numerical studies at very high rapidities [43] but slightly smaller than the theoretical expectation $d = 4.88$ [32, 33]. In previous numerical studies [39, 40, 42], an even smaller value of $d \sim 4.1$ was obtained. We have checked that this is due to the fact that the rapidity region for the fit in our case corresponds to much larger Y .

For the case of a running coupling constant, an exponential fit can be done only for a very limited Y -region. For example, for $Y \sim 10$ we find a logarithmic slope ~ 0.28 for GBW or MV initial conditions with $Q_0 \sim 1$ GeV, in agreement with the results of [45] but smaller than the values found in [83] (see also [48, 89]). The exponential function (21) is unable to fit the full Y -range. In contrast, the weaker rapidity dependence of (24) does provide a good fit in the full Y -range. The fit to (24) yields $\Delta' \simeq 3.2$, while the theoretical expectation [32, 33] is slightly larger, $\Delta' = 3.6$. We finally note that in [47] the Y -derivative of $\ln Q_s^2(Y)$ has been found numerically to be proportional to $\sqrt{\alpha_s(Q_s(Y))}$ in a much more restricted range of Y . We have been unable to fit our results over the full Y -range to the corresponding Y -dependence, $Q_s^2(Y) \propto \exp Y^{2/3}$.

We have found very little sensitivity of the values of Δ and Δ' to the fitting region, provided Y was chosen large enough. Our fits typically started at $Y \sim 15$ where the asymptotic behaviour is approached, and explored the highest rapidities numerically accessible. Also, our results for running coupling do not depend on the choice of the kernel $K1$, $K2$ or $K3$, on the initial condition or on the value of $\bar{\alpha}_0$. However, the AS initial condition with $c = 0.84$ is not included in our study since it does not approach the asymptotics within the numerically accessible rapidity range.

In References [33, 35–37, 45] sub-leading terms in the Y -behaviour of Q_s have been presented. A form of the type $d \ln Q_s^2(Y)/dY = \bar{\alpha}_s a - bY^{-1} + cY^{-3/2}/(2\sqrt{\bar{\alpha}_s})$ has been proposed in the fixed coupling case, with $a = 4.88$, $b = 2.39$ and $c = 2.74$. This function contains all terms for the Y -evolution of the saturation scale that are universal i.e. independent of the initial condition (see also [90] for a comparison of solutions of BK to this functional form). The constant term corresponds to Equation (21). We have used this functional form to fit the results of fixed coupling evolution on $d \ln Q_s^2(Y)/dY$ for different rapidity regions within $Y = 5 \div 40$ (72) for $\bar{\alpha}_s = 0.4$ (0.2), for the GBW and MV initial conditions. First, we have used our definition of the saturation scale

(13) with $\kappa = 1/2$. From a simple comparison to the proposed expression (using the theoretical coefficients provided in [37]), we are able to clearly identify in our numerical results the presence of the first two terms. On the contrary, the presence of the third term is disfavoured. Fitting our numerical results to the first plus second terms, the value of a we find, $a \simeq 4.9$, is quite stable with respect to variations of the fitting region. It is higher than the value of d we extract with only the linear term (21), $d \simeq 4.57$, and closer to the theoretical expectation $d = 4.88$ [32,33]. In this two-parameter fit we get a value of $b \simeq 2.4 \div 2.5$, varying slightly with the Y -region of the fit. This value is quite close to the theoretical expectation 2.39. On the other hand, in a three-parameter fit the values of b and c we extract are very unstable (even changing signs) with respect to variations of the lower limit of the fitting region between $Y = 5$ and 20. We have also tried to get the value of c from a fit to $d/dY[Y d \ln Q_s^2(Y)/dY] = \bar{\alpha}_s a - cY^{-3/2}/(4\sqrt{\bar{\alpha}_s})$. While we find again a value of $a \simeq 4.9$, the value of c turns out to depend, as in the previous analysis, considerably on the fitted Y -region. Secondly, we have used the definition of the saturation scale (13) but now with $\kappa = 0.01$ (i.e. we define Q_s in a point in which the dipole scattering probability is far from its unitarity limit). In this case, a simple comparison to the proposed expression using the theoretical coefficients provided in [37] allows to clearly identify in our numerical results the presence of the three terms. Still, a three-parameter fit to our numerical results does not provide values of b and c stable with respect to changes in the fitting region. This influence of the definition of the saturation scale on the determination of the sub-leading corrections to its Y -behaviour is consistent with the finding in [90].

5.4 Nuclear size dependence of the saturation scale

The nuclear size enters the initial condition. The question is whether the BK evolution modifies or preserves this initial A -dependence. For realistic nuclei, the impact parameter is likely to have an important effect on this A -dependence. This has been examined partially in [50,51]. However, the question is already of interest for the case without impact parameter dependence [34,39,40], which we study here.

Let us first assume some arbitrary A -dependence which we include in the initial condition by the rescaling factor

$$r^2 \longrightarrow h r^2 \tag{25}$$

(this is true for GBW and AS initial conditions but not for MV due to the presence of the logarithm; however, the numerical results for the A -dependence obtained with MV initial conditions are, for all purposes, equivalent to those with GBW). Here, h contains the information about the nuclear size, and Equation (20) reads

$$\frac{\partial \ln [Q_s^2(Y)/\Lambda^2]}{\partial Y} = d\bar{\alpha}_s(\sqrt{h} Q_s(Y)). \quad (26)$$

In the case of a fixed coupling constant, the dilatation invariance of the BK equation (2) allows to scale out any nuclear dependence included in the initial condition. Thus, the A -dependence of the saturation scale is unaffected by evolution. To explore the case of a running coupling constant, we use the one-loop expression for α_s and write

$$Q_s^2(Y) = \frac{\Lambda^2}{h} \exp \sqrt{(\Delta')^2 Y + \ln^2 \left[\frac{h Q_s^2(Y=0)}{\Lambda^2} \right]}. \quad (27)$$

Multiplying by h for the nucleus to undo the rescaling, and setting $h = 1$ for the proton, we get

$$\frac{Q_{sA}^2(Y)}{Q_{sp}^2(Y)} = \exp \left\{ \sqrt{(\Delta')^2 Y + \ln^2 \left[\frac{h Q_s^2(Y=0)}{\Lambda^2} \right]} - \sqrt{(\Delta')^2 Y + \ln^2 \left[\frac{Q_s^2(Y=0)}{\Lambda^2} \right]} \right\}. \quad (28)$$

If we assume the hierarchy

$$(\Delta')^2 Y \gg \ln^2 \left[\frac{h Q_s^2(Y=0)}{\Lambda^2} \right] \gg \ln^2 \left[\frac{Q_s^2(Y=0)}{\Lambda^2} \right], \quad (29)$$

so $A \gg 1$, we find

$$\ln \frac{Q_{sA}^2(Y)}{Q_{sp}^2(Y)} \simeq \frac{\ln^2 \left[\frac{h Q_s^2(Y=0)}{\Lambda^2} \right]}{2\sqrt{(\Delta')^2 Y}}. \quad (30)$$

Here, $h Q_s^2(Y=0)$ is the initial saturation momentum for the nucleus, and Equation (30) coincides with Equation (44) of [34] with $(\Delta')^2$ as defined below Equation (24) (see also [47,64,91] for related discussions). This result suggests that any information about the initial A -dependence of the saturation scale is gradually lost during evolution: albeit at extremely large rapidities, all hadronic targets look the same. Usually, one assumes an $A^{1/3}$ -dependence of the saturation scale for the initial condition [6,7], $h \propto A^{1/3}$. However, other A -dependencies have been proposed e.g. [92].

Figure 7 shows that fixed coupling evolution preserves the A -dependence of the saturation scale irrespective of whether this dependence is $\propto A^{1/3}$ as for the GBW or MV initial conditions (which produces numerical results for the A -dependence which

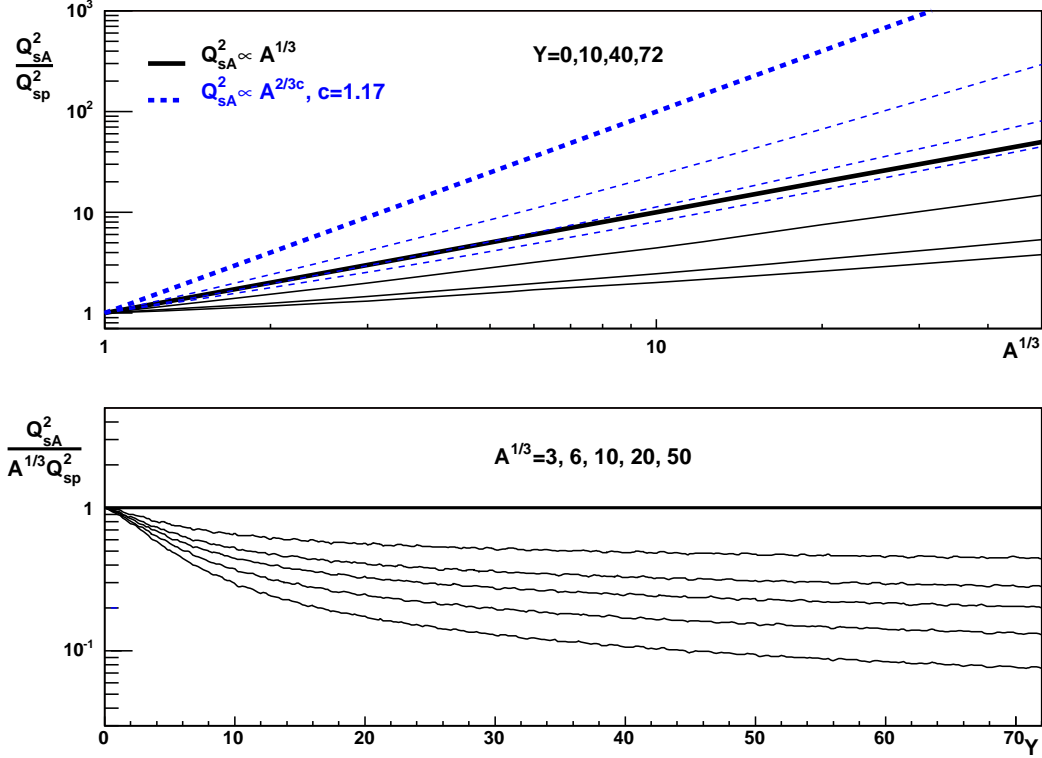


Figure 7: Upper plot: Q_{sA}^2/Q_{sp}^2 versus $A^{1/3}$ for initial conditions GBW ($Q_{sA}^2(Y=0) \propto A^{1/3}$, solid) and AS with $c = 1.17$ ($Q_{sA}^2(Y=0) \propto A^{2/3c}$, dashed lines); thick lines are the results for $Y = 0$ in the running coupling case and for all rapidities in fixed coupling; for running coupling, different rapidities $Y = 10, 40$ and 72 (thin lines) are shown from top to bottom for each initial condition. Lower plot: $Q_{sA}^2/(A^{1/3}Q_{sp}^2)$ versus Y for GBW with $A^{1/3} = 3, 6, 10, 20$ and 50 with the same line convention as the upper plot (the results for fixed coupling have been obtained for $Y < 36$ and extrapolated as a constant equal to 1). In all plots $\bar{\alpha}_0 = 0.4$ and in the running coupling case the kernel $K1$ has been used.

are very close to those obtained for GBW), or whether it differs from $\propto A^{1/3}$ due to an anomalous dimension included e.g. in the AS initial condition. On the other hand, running coupling evolution is seen to reduce the A -dependence with increasing rapidity. We find that if fitted in a wide rapidity range, the dependence of $\ln [Q_{sA}^2(Y)/Q_{sp}^2(Y)]$ on Y is $\sim Y^{-0.4}$. However, for large values of A and Y , the decrease with increasing Y is $\propto 1/\sqrt{Y}$ and thus well described by (30) [34].

Combining the rescaling argument based in (25) with the observation that the DLL solution is approached for small r or large transverse momentum k , one is led to an interesting implication for the large- k behaviour of the ratios of gluon densities in

nuclei over nucleon (or central over peripheral nucleus) [43, 68–70]. In fixed coupling evolution the rescaling of the initial condition (25) trivially implies the same rescaling in the evolved solution, which we will consider to be DLL for sufficiently large k . Thus one gets for the ratio R of the gluon densities in transverse momentum space for nuclei over nucleon

$$R \simeq \left[\frac{\ln(k^2/\Lambda^2) - \ln h}{\ln(k^2/\Lambda^2)} \right]^{-3/4} \exp \left\{ b(Y) \left[\sqrt{\ln(k^2/\Lambda^2) - \ln h} - \sqrt{\ln(k^2/\Lambda^2)} \right] \right\}. \quad (31)$$

This ratio tends very slowly to 1 for $k \rightarrow \infty$. We have checked that the results of this formula agree with the numerical computations in [43] and thus it provides justification to the apparent absence of a return to the collinear limit, $R = 1$ at $k \rightarrow \infty$, found in this reference for the largest studied k -values.

6 Conclusions

The inclusion of a running coupling constant may be expected to account for important next-to-leading-log effects in the BK equation, as has been previously the case for BFKL. This motivates the present numerical study of the BK equation without impact parameter dependence. Our main results are insensitive to details of the implementation of running coupling effects, the infrared regulation of the coupling constant and the choice of initial conditions which are evolved. They can be summarized as follows:

1. The rapidity dependence of the saturation momentum is much faster for fixed coupling constant than for the running one, as observed previously [42, 44, 46, 47]. It is well described by $Q_s^2(Y) \propto \exp(\bar{\alpha}_s d Y)$ for fixed coupling and by $Q_s^2(Y) \propto \exp(\Delta' \sqrt{Y + \bar{X}})$ for running coupling. For large rapidities, we find $d \simeq 4.57$ which is slightly smaller than the theoretical expectation $d = 4.88$ [32, 33]. For running coupling, we find $\Delta' \simeq 3.2$, slightly smaller than the expected value $\Delta' \simeq 3.6$ [32, 33, 45]. For a very limited region of Y , a fit to the exponential form $Q_s^2(Y) \propto \exp(D Y)$ works even for running coupling, but it cannot account for the entire Y -range. For the fixed coupling case, we have checked the existence of the sub-leading terms in the Y -dependence of the saturation scale proposed in [33, 35–37]. As found in [90], their precise determination depends on the definition of the saturation scale.

2. For sufficiently large rapidity, the solution of the BK equation with fixed coupling is known to show scaling [39, 41, 43]. We confirm scaling for the running coupling case in agreement with [46, 47]. The approach to the scaling solution is faster with fixed than with running coupling.
3. As observed previously [46] and at variance with analytical estimates [32, 33, 45], the behaviour of $N(r)$ at small r differs for the cases of fixed and running coupling. For small $r < 1/Q_s(Y)$, forms of the type $(r Q_s)^{2\gamma} \ln(C r Q_s)$ [33] describe the solutions at sufficiently high rapidity, where γ , defined in a Y -independent fitting region, is $\simeq 0.65$ for the fixed coupling constant but $\gamma \sim 0.85$ for running coupling. These values are for the limit $Y \rightarrow \infty$.
4. Arguments in [32, 33] suggest a lower limit to the scaling window $r Q_s(Y) \sim \Lambda_{QCD}/Q_s(Y)$ below which $N(r)$ returns to the perturbative double-leading-logarithmic expression. Remarkably, the scaling forms (14) proposed in [33, 45] give good fits to the solutions of BK even outside the scaling window, for $r < \Lambda/Q_s^2(Y)$, $\Lambda \sim 0.2$ GeV. Hence, it is not possible to establish numerically the limit of the scaling region as a deviation from scaling. However, the double-leading-log approximation provides an equally good description of the numerical solution in the r -region below the scaling window.
5. For fixed coupling, the scale invariance of the kernel preserves any A -dependence of the initial condition during BK evolution. For running coupling and for very large energies and nuclear sizes, we have re-derived and checked numerically Equation (30): the A -dependence decreases with increasing rapidity like $1/\sqrt{Y}$ [34].

The above results have been established by evolving over many orders of magnitude in energy. Thus, any phenomenological application of these findings has to assume that initial conditions can be fixed at (and perturbatively evolved from) a sufficiently small energy scale for the non-linear evolution to be effective in an experimentally accessible regime. Moreover, phenomenology based on the BK equation will face at least some of the problems known from applications of BFKL such as the question of whether and how to implement kinematical cuts for gluon emission. Despite these caveats, it is interesting to compare the numerical results found here to the general trends in

the data. A comparison of saturation-inspired parameterizations with data on lepton-proton, lepton-nucleus and nuclear collisions at high energies suggests a saturation scale $Q_{sA}^2 \propto A^\alpha \exp(DY)$ with $D \simeq 0.29$ [88] and $\alpha \simeq 4/9 > 1/3$ [57] (for related phenomenological studies, see [55,56]).

Our results allow to discuss to which extent existing data, showing geometric scaling, differ from the asymptotic BK scaling behaviour. In particular, the strong A -dependence of the saturation scale seen in the data indicates, at variance with the result from the BK scaling solution with running coupling, that the properties of the initial nuclear condition have not yet been washed out by non-linear small- x evolution. The kinematic range of the lepton-nucleus data studied in [56,57] is too small to test this evolution. Also, the exponential Y -dependence of the saturation scale with $D \sim 0.3$ seen in the data can appear naturally from BK evolution of reasonable initial conditions over some units in rapidity in the running coupling case. But this value of D is not a property of the asymptotic solution for running coupling. For fixed coupling, it can only be obtained with unrealistically small values of the coupling constant.

None of these facts contradicts non-linear BK evolution – they simply illustrate that the evolution observed in experimental data has not yet reached its asymptotic behaviour. To further advance our understanding of saturation effects in QCD dynamics at high energies, both theoretical and experimental studies are required. In the context of the BK equation, this requires the study of solutions under more realistic conditions. In particular, the impact parameter dependence may have a significant effect on the A -dependence of the saturation scale, a point which we plan to study in the future. On the experimental side, the forward rapidity measurements at the BNL Relativistic Heavy Ion Collider RHIC give access to a kinematic window interesting for small- x evolution studies. These studies are at the very beginning. Also, in the near future measurements at the CERN Large Hadron Collider LHC will provide more stringent tests of small- x evolution, extending the kinematic reach by at least three orders of magnitude further down in the momentum fraction x .

Acknowledgments: We thank R. Baier, J. Bartels, M. A. Braun, E. Iancu, A. H. Mueller and A. Sabio Vera for useful discussions and comments. We are grateful to K. Golec-Biernat for a critical reading of the manuscript and many helpful remarks. Special thanks are due to A. Kovner, who participated in an early stage of this work

and made numerous useful suggestions about the manuscript. J. L. A. and J. G. M. thank CERN Theory Division for hospitality, and acknowledge financial support by the Ministerio de Educación y Ciencia of Spain (grant no. AP2001-3333) and the Fundação para a Ciência e a Tecnologia of Portugal (contract SFRH/BPD/12112/2003) respectively.

References

- [1] *QCD Perspectives on Hot and Dense Matter (NATO Science Series II: Mathematics, Physics and Chemistry, Vol. 87)*, Eds. J.-P. Blaizot and E. Iancu, Kluwer 2002.
- [2] E. A. Kuraev, L. N. Lipatov and V. S. Fadin, *Sov. Phys. JETP* **45**, 199 (1977) [*Zh. Eksp. Teor. Fiz.* **72**, 377 (1977)].
- [3] I. I. Balitsky and L. N. Lipatov, *Sov. J. Nucl. Phys.* **28**, 822 (1978) [*Yad. Fiz.* **28**, 1597 (1978)].
- [4] L. V. Gribov, E. M. Levin and M. G. Ryskin, *Phys. Rept.* **100**, 1 (1983).
- [5] A. H. Mueller and J. w. Qiu, *Nucl. Phys. B* **268**, 427 (1986).
- [6] L. D. McLerran and R. Venugopalan, *Phys. Rev. D* **49**, 2233 (1994).
- [7] L. D. McLerran and R. Venugopalan, *Phys. Rev. D* **49**, 3352 (1994).
- [8] L. D. McLerran and R. Venugopalan, *Phys. Rev. D* **50**, 2225 (1994).
- [9] J. Jalilian-Marian, A. Kovner, L. D. McLerran and H. Weigert, *Phys. Rev. D* **55**, 5414 (1997).
- [10] J. Jalilian-Marian, A. Kovner, A. Leonidov and H. Weigert, *Phys. Rev. D* **59**, 014014 (1999).
- [11] J. Jalilian-Marian, A. Kovner, A. Leonidov and H. Weigert, *Phys. Rev. D* **59**, 034007 (1999) [Erratum-ibid. *D* **59**, 099903 (1999)].
- [12] A. Kovner and J. G. Milhano, *Phys. Rev. D* **61**, 014012 (2000).
- [13] E. Iancu, A. Leonidov and L. D. McLerran, *Nucl. Phys. A* **692**, 583 (2001).

- [14] E. Iancu, A. Leonidov and L. D. McLerran, Phys. Lett. B **510**, 133 (2001).
- [15] E. Ferreira, E. Iancu, A. Leonidov and L. McLerran, Nucl. Phys. A **703**, 489 (2002).
- [16] W. Buchmuller and A. Hebecker, Nucl. Phys. B **476**, 203 (1996).
- [17] A. L. Ayala, M. B. Gay Ducati and E. M. Levin, Nucl. Phys. B **493**, 305 (1997).
- [18] I. Balitsky, Nucl. Phys. B **463**, 99 (1996).
- [19] H. Weigert, Nucl. Phys. A **703**, 823 (2002).
- [20] Y. V. Kovchegov, Phys. Rev. D **60**, 034008 (1999).
- [21] N. N. Nikolaev and B. G. Zakharov, Z. Phys. C **49**, 607 (1991).
- [22] A. H. Mueller, Nucl. Phys. B **415**, 373 (1994).
- [23] A. H. Mueller and B. Patel, Nucl. Phys. B **425**, 471 (1994).
- [24] A. Kovner, J. G. Milhano and H. Weigert, Phys. Rev. D **62**, 114005 (2000).
- [25] A. H. Mueller, Phys. Lett. B **523**, 243 (2001).
- [26] J. P. Blaizot, E. Iancu and H. Weigert, Nucl. Phys. A **713**, 441 (2003).
- [27] E. Iancu and A. H. Mueller, Nucl. Phys. A **730**, 460 (2004).
- [28] A. Kovner and U. A. Wiedemann, Phys. Rev. D **64**, 114002 (2001).
- [29] M. Braun, Eur. Phys. J. C **16**, 337 (2000).
- [30] J. Bartels, L. N. Lipatov and G. P. Vacca, arXiv:hep-ph/0404110.
- [31] E. Levin and K. Tuchin, Nucl. Phys. B **573**, 833 (2000).
- [32] E. Iancu, K. Itakura and L. McLerran, Nucl. Phys. A **708**, 327 (2002).
- [33] A. H. Mueller and D. N. Triantafyllopoulos, Nucl. Phys. B **640**, 331 (2002).
- [34] A. H. Mueller, Nucl. Phys. A **724**, 223 (2003).
- [35] S. Munier and R. Peschanski, Phys. Rev. Lett. **91**, 232001 (2003).

- [36] S. Munier and R. Peschanski, Phys. Rev. D **69**, 034008 (2004).
- [37] S. Munier and R. Peschanski, Phys. Rev. D **70**, 077503 (2004).
- [38] M. A. Kimber, J. Kwiecinski and A. D. Martin, Phys. Lett. B **508**, 58 (2001).
- [39] N. Armesto and M. A. Braun, Eur. Phys. J. C **20**, 517 (2001).
- [40] E. Levin and M. Lublinsky, Nucl. Phys. A **696**, 833 (2001).
- [41] M. Lublinsky, Eur. Phys. J. C **21**, 513 (2001).
- [42] K. Golec-Biernat, L. Motyka and A. M. Stasto, Phys. Rev. D **65**, 074037 (2002).
- [43] J. L. Albacete, N. Armesto, A. Kovner, C. A. Salgado and U. A. Wiedemann, Phys. Rev. Lett. **92**, 082001 (2004).
- [44] M. Lublinsky, E. Gotsman, E. Levin and U. Maor, Nucl. Phys. A **696**, 851 (2001).
- [45] D. N. Triantafyllopoulos, Nucl. Phys. B **648**, 293 (2003).
- [46] M. A. Braun, Phys. Lett. B **576**, 115 (2003).
- [47] K. Rummukainen and H. Weigert, Nucl. Phys. A **739**, 183 (2004).
- [48] K. Kutak and A. M. Stasto, arXiv:hep-ph/0408117.
- [49] A. Kovner and U. A. Wiedemann, Phys. Rev. D **66**, 051502 (2002).
- [50] K. Golec-Biernat and A. M. Stasto, Nucl. Phys. B **668**, 345 (2003).
- [51] E. Gotsman, M. Kozlov, E. Levin, U. Maor and E. Naftali, Nucl. Phys. A **742**, 55 (2004).
- [52] E. Iancu and A. H. Mueller, Nucl. Phys. A **730**, 494 (2004).
- [53] A. H. Mueller and A. I. Shoshi, Nucl. Phys. B **692**, 175 (2004).
- [54] E. Iancu, A. H. Mueller and S. Munier, arXiv:hep-ph/0410018.
- [55] A. M. Stasto, K. Golec-Biernat and J. Kwiecinski, Phys. Rev. Lett. **86**, 596 (2001).
- [56] A. Freund, K. Rummukainen, H. Weigert and A. Schafer, Phys. Rev. Lett. **90**, 222002 (2003).

- [57] N. Armesto, C. A. Salgado and U. A. Wiedemann, arXiv:hep-ph/0407018.
- [58] E. Gotsman, E. Levin, M. Lublinsky and U. Maor, Eur. Phys. J. C **27**, 411 (2003).
- [59] K. J. Eskola, H. Honkanen, V. J. Kolhinen, J. w. Qiu and C. A. Salgado, Nucl. Phys. B **660**, 211 (2003).
- [60] N. Armesto, Acta Phys. Polon. B **35**, 213 (2004).
- [61] M. Gyulassy and L. McLerran, arXiv:nucl-th/0405013.
- [62] D. Kharzeev and M. Nardi, Phys. Lett. B **507**, 121 (2001).
- [63] D. Kharzeev and E. Levin, Phys. Lett. B **523**, 79 (2001).
- [64] D. Kharzeev, E. Levin and M. Nardi, arXiv:hep-ph/0408050.
- [65] M. A. Braun and C. Pajares, arXiv:hep-ph/0405203.
- [66] M. A. Braun, Phys. Lett. B **599**, 269 (2004).
- [67] D. Kharzeev, E. Levin and L. McLerran, Phys. Lett. B **561**, 93 (2003).
- [68] R. Baier, A. Kovner and U. A. Wiedemann, Phys. Rev. D **68**, 054009 (2003).
- [69] D. Kharzeev, Y. V. Kovchegov and K. Tuchin, Phys. Rev. D **68**, 094013 (2003).
- [70] D. Kharzeev, Y. V. Kovchegov and K. Tuchin, arXiv:hep-ph/0405045.
- [71] V. S. Fadin and L. N. Lipatov, Phys. Lett. B **429**, 127 (1998).
- [72] M. Ciafaloni and G. Camici, Phys. Lett. B **430**, 349 (1998).
- [73] D. A. Ross, Phys. Lett. B **431**, 161 (1998).
- [74] Y. V. Kovchegov and A. H. Mueller, Phys. Lett. B **439**, 428 (1998).
- [75] N. Armesto, J. Bartels and M. A. Braun, Phys. Lett. B **442**, 459 (1998).
- [76] J. R. Andersen and A. Sabio Vera, Phys. Lett. B **567**, 116 (2003).
- [77] J. R. Andersen and A. Sabio Vera, Nucl. Phys. B **679**, 345 (2004).
- [78] S. J. Brodsky, V. S. Fadin, V. T. Kim, L. N. Lipatov and G. B. Pivovarov, JETP Lett. **70**, 155 (1999).

- [79] C. R. Schmidt, Phys. Rev. D **60**, 074003 (1999).
- [80] J. R. Forshaw, D. A. Ross and A. Sabio Vera, Phys. Lett. B **455**, 273 (1999).
- [81] M. Ciafaloni, D. Colferai, G. P. Salam and A. M. Stasto, Phys. Lett. B **587**, 87 (2004).
- [82] G. Altarelli, R. D. Ball and S. Forte, Nucl. Phys. B **674**, 459 (2003).
- [83] V. A. Khoze, A. D. Martin, M. G. Ryskin and W. J. Stirling, arXiv:hep-ph/0406135.
- [84] A. H. Mueller, Phys. Lett. B **396**, 251 (1997).
- [85] A. Babansky and I. Balitsky, Phys. Rev. D **67**, 054026 (2003).
- [86] L. N. Lipatov, Sov. Phys. JETP **63**, 904 (1986) [Zh. Eksp. Teor. Fiz. **90**, 1536 (1986)].
- [87] J. C. Collins and J. Kwiecinski, Nucl. Phys. B **316**, 307 (1989).
- [88] K. Golec-Biernat and M. Wusthoff, Phys. Rev. D **59**, 014017 (1999).
- [89] G. Chachamis, M. Lublinsky and A. Sabio Vera, arXiv:hep-ph/0408333.
- [90] K. Golec-Biernat, arXiv:hep-ph/0408255.
- [91] E. M. Levin and M. G. Ryskin, Yad. Fiz. **45**, 234 (1987) [Sov. J. Nucl. Phys. **45**, 150 (1987)].
- [92] E. Levin and K. Tuchin, Nucl. Phys. A **693**, 787 (2001).